Changes in Distribution of Nuclear Matrix Antigens during the Mitotic Cell Cycle

NATHALIE CHALY, TREVOR BLADON,* GEORGE SETTERFIELD,* JUDY E. LITTLE, J. GORDIN KAPLAN,‡ and DAVID L. BROWN
Departments of Biology, University of Ottawa and Carleton University,* Ottawa, and Department of Biochemistry,‡ University of Alberta, Edmonton, Canada

ABSTRACT   We examined the distribution of nonlamin nuclear matrix antigens during the mitotic cell cycle in mouse 3T3 fibroblasts. Four monoclonal antibodies produced against isolated nuclear matrices were used to characterize antigens by the immunoblotting of isolated nuclear matrix preparations, and were used to localize the antigens by indirect immunofluorescence. For comparison, lamins and histones were localized using human autoimmune antibodies. At interphase, the monoclonal antibodies recognized non-nucleolar and nonheterochromatin nuclear components. Antibody P1 stained the nuclear periphery homogeneously, with some small invaginations toward the interior of the nucleus. Antibody I1 detected an antigen distributed as fine granules throughout the nuclear interior. Monoclonals PI1 and PI2 stained both the nuclear periphery and interior, with some characteristic differences. During mitosis, P1 and I1 were chromosome-associated, whereas PI1 and PI2 dispersed in the cytoplasm. Antibody P1 heavily stained the periphery of the chromosome mass, and we suggest that the antigen may play a role in maintaining interphase and mitotic chromosome order. With antibody I1, bright granules were distributed along the chromosomes and there was also some diffuse internal staining. The antigen to I1 may be involved in chromatin/chromosome higher-order organization throughout the cell cycle. Antibodies PI1 and PI2 were redistributed independently during prophase, and dispersed into the cytoplasm during prometaphase. Antibody PI2 also detected antigen associated with the spindle poles.

The nuclear matrix is a complex biochemical fraction consisting of nonhistone nuclear proteins and small quantities of DNA and RNA. It is obtained by sequential extraction of isolated interphase nuclei with low- and high-salt buffers, detergents, and DNAse and RNAse. Structurally, the nuclear matrix comprises the peripheral nuclear pore complex—lamina, an internal fibrogranular network and residual nucleoli. Part of the matrix has been envisaged as an interphase "nuclear skeleton" on which nuclear functions such as DNA replication, RNA transcription and processing, virus replication, and hormone response can be ordered (see references 1–3 for reviews).

Several studies have suggested that the nuclear matrix is involved in mitosis (4–7). Recent work (8, 9) has also indicated a potential role for the nuclear matrix in the organization of mitotic chromosomes per se. To examine the distribution of individual nuclear matrix polypeptides throughout the cell cycle, we used monoclonal antibodies against isolated nuclear matrices in an immunofluorescence study of mouse 3T3 fibroblasts.

MATERIALS AND METHODS

Cell Culture: Mouse 3T3 fibroblasts were cultured at 37°C with 5% CO_2 in Dulbecco's modified Eagle's medium with 10% fetal calf serum, 100 U/ml penicillin, 100 µg/ml streptomycin, and 0.25 µg/ml fungizone. Mouse myeloma Sp2/0 cells were grown in the same conditions but in 10% CO_2.

Production of Monoclonal Antibodies: Nuclear matrices from resting mouse splenic or bovine lymph node lymphocytes were isolated as previously described (10). BALB/c-BYJ mice received a total of 400 µg/mouse of mouse or bovine lymphocyte nuclear matrix in four injections at 10-d intervals. Fusion, cloning, and ascites fluid production were carried out according to the protocol of Kennett et al. (11). Hybrids were screened by an indirect immunofluorescence assay. Mouse 3T3 cells were grown on coverslips (c.s.),[1] fixed in cold 95% ethanol, and air-dried. Small volumes of supernatant were

---

[1] *Abbreviations used in this paper:* c.s., coverslip; FITC, fluorescein isothiocyanate.

applied for 30 min; the c.s. were rinsed in phosphate-buffered saline (PBS), pH 7.0, flooded with fluorescein isothiocyanate (FITC)-conjugated goat anti-mouse Ig for 30 min, washed in PBS, and mounted in 50% glycerol-PBS with 0.1% p-phenylenediamine to retard fluorescence bleaching.

Immunoblotting: Lymphocyte nuclear matrix proteins were separated in SDS polyacrylamide gels according to Brasch (12) and were transferred electrophoretically to nitrocellulose (Bio-Rad Laboratories, Richmond, CA) by a modification of the method of Burnette (13). The electrode buffer contained 192 mM glycine and 25 mM Trizma base. The total transferred proteins were visualized directly by staining a strip of the nitrocellulose sheet with amido black. Molecular weights were estimated by comparison with high- and low-molecular-weight standard kits (Bio-Rad Laboratories, Mississauga, Ont.).

For immunostaining, the nitrocellulose sheet was incubated at room temperature in 3% gelatin in PBS, pH 7.0, to block nonspecific staining. Nitrocellulose strips were then incubated with ascites fluid at 4°C for 16 h, at the following dilutions: P1, 1:1000; PI1, 1:200; PI2, 1:200. Detection used horseradish peroxidase-conjugated goat anti-mouse IgM (1:400) (Cappel Laboratories, Inc., Cochranville, PA) and diaminobenzidine (Polysciences, Inc., Markham, Ont.).

Immunofluorescent Staining: Mouse 3T3 fibroblasts were grown on c.s. and fixed in 3% paraformaldehyde-PBS, pH 7.0, for 5 min at room temperature. They were reduced in sodium borohydride in PBS, permeabilized for 20 min in 0.2% Triton X-100 in PBS, washed in PBS, drained, and flooded with 1° antibody. Control samples were flooded with PBS. The c.s. were incubated for 45 min, drained, washed in PBS, flooded with 2° antibody, and incubated for 45 min. After washing in PBS, the c.s. were placed in Hoechst 33258 (American Hoechst Corp., San Diego, CA) (1.5 μg/ml in PBS, pH 7.0) and then mounted in 50% glycerol-PBS with p-phenylenediamine.

Double Immunofluorescence Staining: After fixation, permeabilization and washing in PBS as above, the c.s. were placed for 20 min in 0.15% gelatin in PBS and washed three times for 10 min in PBS. The antibodies were then applied as follows: first 1° antibody, 45 min; three times for 4 min in PBS; first 2° antibody, 45 min; three times for 4 min in PBS; second 1° antibody, 45 min; three times for 4 min in PBS; second 2° antibody, 45 min; three times for 4 min in PBS; 2 min in Hoechst 33258; mount in glycerol-PBS.

The following antibodies were used, at the dilution indicated:

1° ANTIBODIES: Monoclonal antibodies to nuclear matrix, ascites fluid: P1, 1:250; I1, 1:100; PI1, 1:500; PI2, 1:750.

Antihistone (1:200) was a previously characterized serum from a patient with an autoimmune disease, kindly supplied by Dr. M. J. Fritzler, University of Calgary. Antilamin (1:400) was a serum from a patient with scleroderma, provided by Dr. M. Kirschner (14).

2° ANTIBODIES: FITC-conjugated goat anti-mouse IgG (H+L) (1:75–1:100) and tetramethylrhodamine isothiocyanate-conjugated goat anti-mouse IgG (H+L) (1:75) (Cappel Laboratories, Inc.); FITC-conjugated goat anti-mouse IgG, gamma chain-specific (1:80), and FITC-conjugated goat anti-mouse IgM, mu chain-specific (1:80) (Flow Laboratories, Inc., Mississauga, Ont.); tetramethylrhodamine isothiocyanate-conjugated rabbit anti-mouse IgG (H+L) (1:75) (Miles Laboratories, Ltd., Rexdale, Ont.); FITC-conjugated rabbit anti-human IgG (H+L) (1:60) and tetramethylrhodamine isothiocyanate-conjugated rabbit anti-human IgG (H+L) (1:125) (Cedar Laboratories Ltd., Hornby, Ont.).

Microscopy: Preparations were observed with a Zeiss Universal microscope (Carl Zeiss, Inc., New York) equipped for epifluorescent illumination and were photographed on Ilford XP1-400 film.

RESULTS

Selection of Monoclonal Antibodies

We selected 17 hybrids producing antibodies that detected nuclear antigens. The staining patterns of interphase nuclei of 3T3 cells with these antibodies fell into three categories: peripheral (P), internal (I), or both (PI). In this study, we report observations using antibodies P1 and I1, produced against bovine retropharyngeal lymphocyte nuclear matrix, and antibodies PI1 and PI2, produced against mouse splenic lymphocyte nuclear matrix. In an earlier report (15), these antibodies were referred to as 3F5, 5H12, 1G11, and 2F8, respectively. All four antibodies were detected by FITC-conjugated goat anti-mouse IgM, but not by FITC-conjugated goat anti-mouse IgG.

The structures and the polypeptide compositions of the isolated lymphocyte nuclear matrices have been described

previously (10, 16). Fig. 1 shows immunoblotting results with lymphocyte matrices for three of the four monoclonal antibodies used in this study. Antibody P1 detected a triplet of polypeptides in the range of M_r 27,000–31,000 and PI1 a single polypeptide of M_r 60,000. Antibody PI2 detected three components (M_r 35,000, 70,000, and 140,000), which may be related subunits or degradation products. We have been unsuccessful so far in identifying the antigen to I1 by immunoblotting.

Interphase

The antigen detected by P1 was exclusively peripheral in interphase (Fig. 2, *a–c*). Focusing on the midplane of the nucleus showed a relatively uniform staining of the periphery (Fig. 2*b*), with some small irregular projections towards the interior of the nucleus. Focusing on the surface of the same nucleus (Fig. 2*a*) showed that the projections were uneven in size and apparently distributed at random.

The staining pattern with antibody P1 was compared to that with antilamin (Fig. 3, *a* and *b*). Peripheral staining was very prominent with antilamin, but showed no internal projections and was agranular. Furthermore, there was a significant fluorescence in the nuclear interior. The internal staining with antilamin consisted of diffuse non-nucleolar fluorescence and some bright irregular streaks and/or spots.

Antibody I1 stained exclusively the internal region of the nucleus. The stain appeared as specks of fairly uniform size
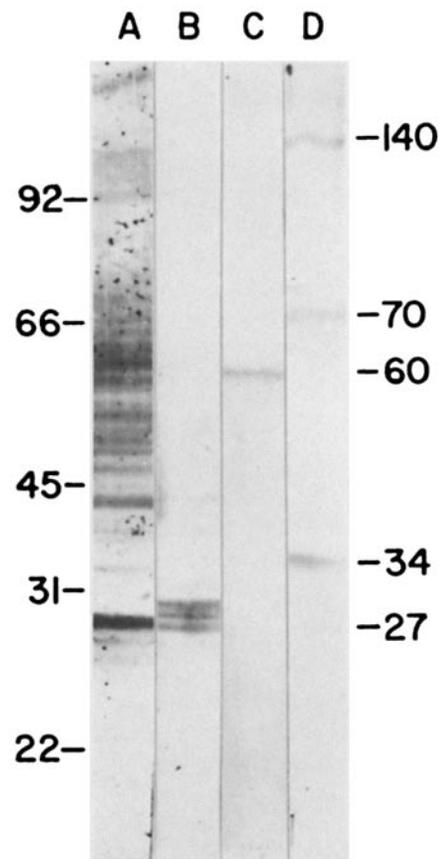
FIGURE 1 Immunoblotting of monoclonal antibodies against lymphocyte matrix polypeptides. Lane A: Total protein transferred to nitrocellulose stained with amido black; Lanes B–D: Antigens detected by antibodies P1 (lane B), PI1 (lane C), and PI2 (lane D). Molecular weights of standards (left) and of antigens (right), × 10^{-3}.
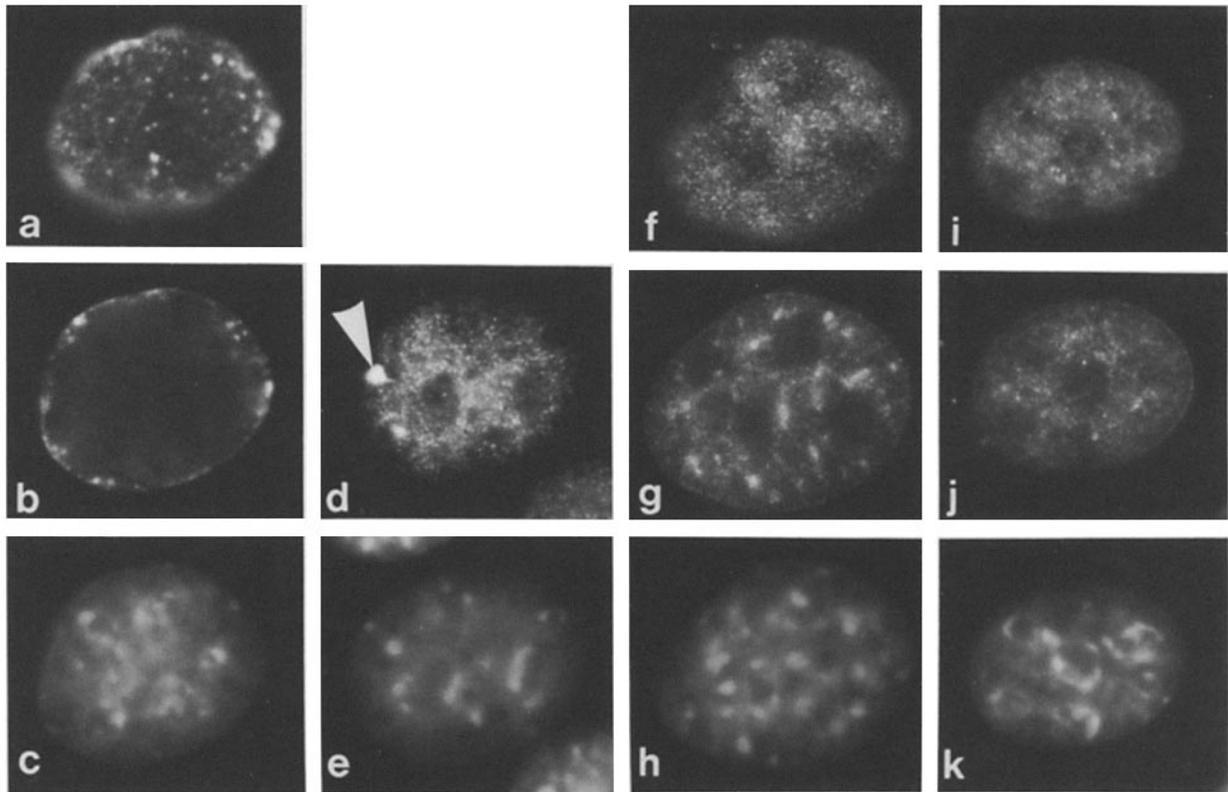
FIGURE 2 Interphase nuclei stained with P1 (a and b), I1 (d), PI1 (f and g) or PI2 (i and j) antibodies, and counterstained with Hoechst (c, e, h, and k, respectively). Antibody I1 stained only the nuclear interior (d) (the arrowhead points to a nucleolus-associated brightly stained mass). Selected focal planes showing nuclear surface (a, f, and i) and interior (b, g, and k) are depicted for the other antibodies. Hoechst micrographs (c, e, h, and k) are at the same focal plane as the micrographs of the interior (b, d, g, and j, respectively). × 1,450.
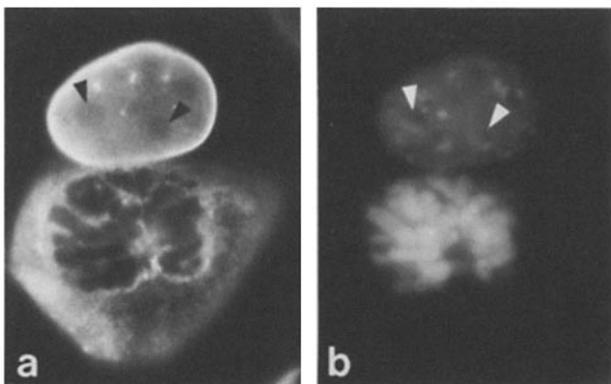
FIGURE 3 Cells in interphase and prometaphase stained with antilamin antibody (a) and Hoechst (b). The interphase nucleus shows intense peripheral staining, some brightly stained internal spots and a diffuse internal stain; nucleoli (arrowheads) are not stained. In prometaphase, fluorescent material is visible in some areas at the periphery of the chromosome mass and the cytoplasm is brightly stained. × 1,450.

and intensity distributed in the regions between nucleoli and heterochromatin bodies, i.e., the interchromatinic region (Fig. 2, d and e). Occasionally, larger bright spots were seen associated with the edge of one or more of the nucleoli.

With antibody PI1, the staining pattern in most nuclei was both peripheral and internal (Figs. 2, f-h, and 4, a-d). In some cases, however, only peripheral staining was observed (Fig. 4, c and d). The peripheral staining was similar in both

situations. Viewed in the midplane of the nucleus (Fig. 2g), the peripheral staining consisted of a discontinuous layer of uniform thickness. In surface view (Fig. 2f), this staining was resolved into evenly distributed coarse granules of uniform size and brightness. The internal staining component was unevenly distributed throughout the nucleoplasm as numerous granules that varied greatly in size and brightness. There was no obvious staining of nucleoli or heterochromatin. A further characteristic of PI1 staining was the presence in the cytoplasm of some cells (Fig. 4, a and b) of a cluster of brightly staining granules of variable size near the nuclear surface.

The interphase staining pattern with antibody PI2 was similar to that with PI1 (Fig. 2, i-k). However, there was little variation in the staining pattern from one cell to another, and the staining was exclusively nuclear in all interphase cells. The peripheral staining consisted of finer, more irregularly sized granules than with PI1, as is clearly seen in Fig. 2i. The internal staining was also somewhat finer (Fig. 2j) and appeared to be more evenly distributed than with PI1.

Mitosis

Cells were identified as to mitotic stage, using primarily DNA staining with Hoechst, according to the following criteria: (a) prophase (Figs. 5 and 6)—from the first sign of chromosome condensation up to the loss of a smooth nuclear outline resulting from the start of nuclear envelope breakdown; (b) prometaphase—from nuclear envelope breakdown to the formation of the metaphase plate; at mid-prometaphase (Fig. 7), chromosomes were oriented radially around a
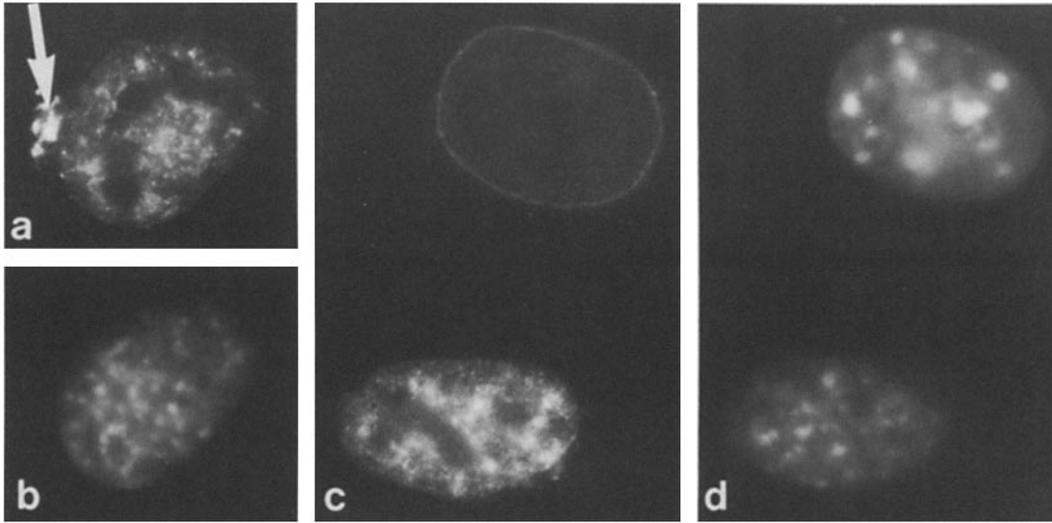
Figure 4 (a and b) Interphase cell stained with PI1 (a) and Hoechst (b) showing a cluster of granules in the cytoplasm near the nuclear periphery (arrow). (c and d) Nuclei in adjacent interphase cells stained with PI1 (c) and Hoechst (d). Although the pattern of DNA fluorescence is similar in the two nuclei, one nucleus shows both peripheral and internal staining whereas the other is stained only peripherally. In both cells, the focus is on the midplane of the nuclei. × 1,450.
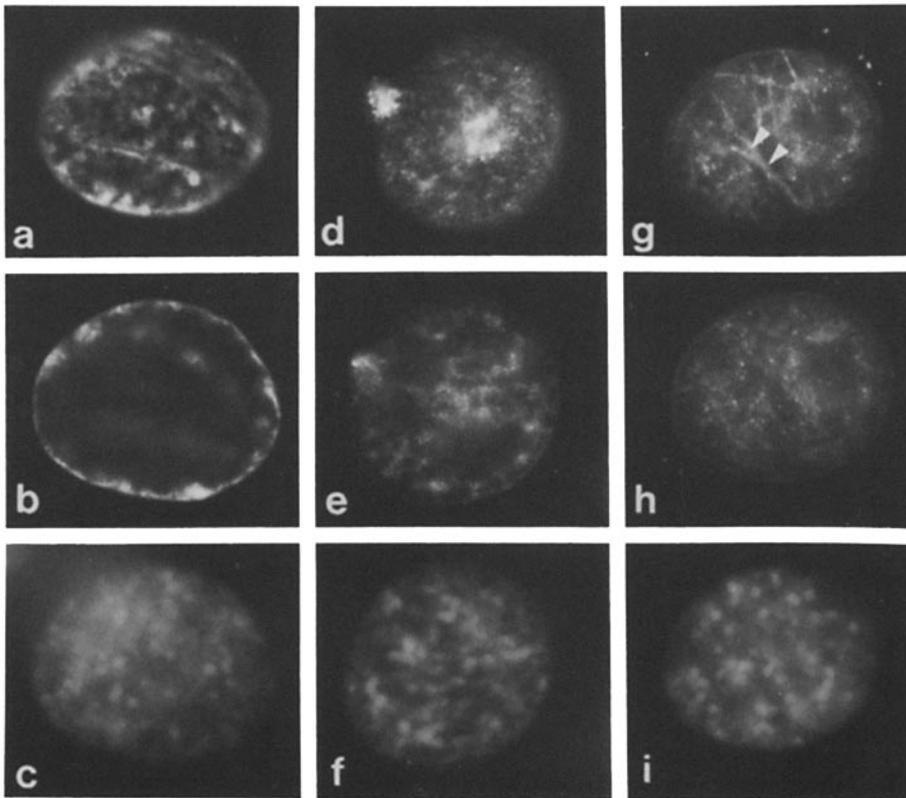
Figure 5 Surface (a, d, and g) and midplane (b, e, and h) views of early prophase nuclei stained with antibodies P1 (a and b), PI1 (d and e), or PI2 (g and h). The same nuclei counterstained with Hoechst are shown in c, f, and i, respectively. Surface invaginations are more numerous in the P1-stained nucleus than at interphase (cf.a, 1a). Two groups of cytoplasmic granules stained by PI1 can be seen near the nuclear surface (d). The peripheral staining by PI2 (h) is diffuse, and the surface shows some "wrinkling" (arrowheads). The internal staining by PI1 (d and e) and PI2 (g and h) is patchy. × 1,450.

nonstaining central space; (c) metaphase (Fig. 8, a–h)—chromosomes aligned at the metaphase plate; (d) anaphase (Fig. 8, i–p)—from the first signs of chromosome separation up to the formation of two chromosome sets at the spindle poles; (e) telophase (Fig. 8, q–x)—individual chromosomes difficult to distinguish, although the chromosome mass as a whole retained a "ropey" appearance; in many instances a midbody was visible by phase-contrast microscopy; (f) early G1 (Fig.

9)—the daughter cells were still connected through the midbody when viewed by phase-contrast microscopy. The paired nuclei were smaller than in surrounding interphase cells, but were otherwise similar in appearance, with a diffuse DNA fluorescence throughout the nucleoplasm and well-defined nucleoli. It should be noted that no squashing was applied to the cell preparations so that the arrangement of chromosomes remained largely undisturbed from that present in living cells.
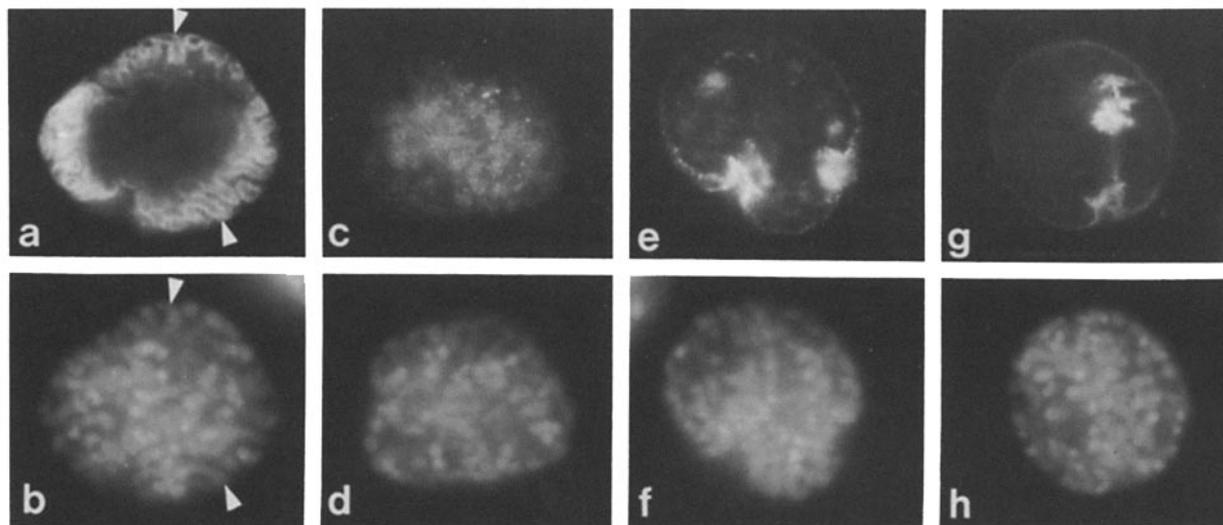
FIGURE 6 Mid-prophase nuclei stained with P1 (a), I1 (c), PI1 (e), or PI2 (g) antibodies and counterstained with Hoechst (b, d, f and h, respectively). (a and b) The chromosome segments at the periphery of the nucleus (arrowheads) (b) are coated with antibody P1 (a). Internal segments of chromosomes are unstained. (c and d) Chromosome segments throughout the nucleus are associated with fine granules of stain. (e and f) The internal staining by PI1 is patchy. The nuclear periphery with two involutions is outlined by granular stain. (g and h) Internal staining by PI2 is not evident at this stage. The peripheral staining is diffuse and shows two involutions. × 1,450.
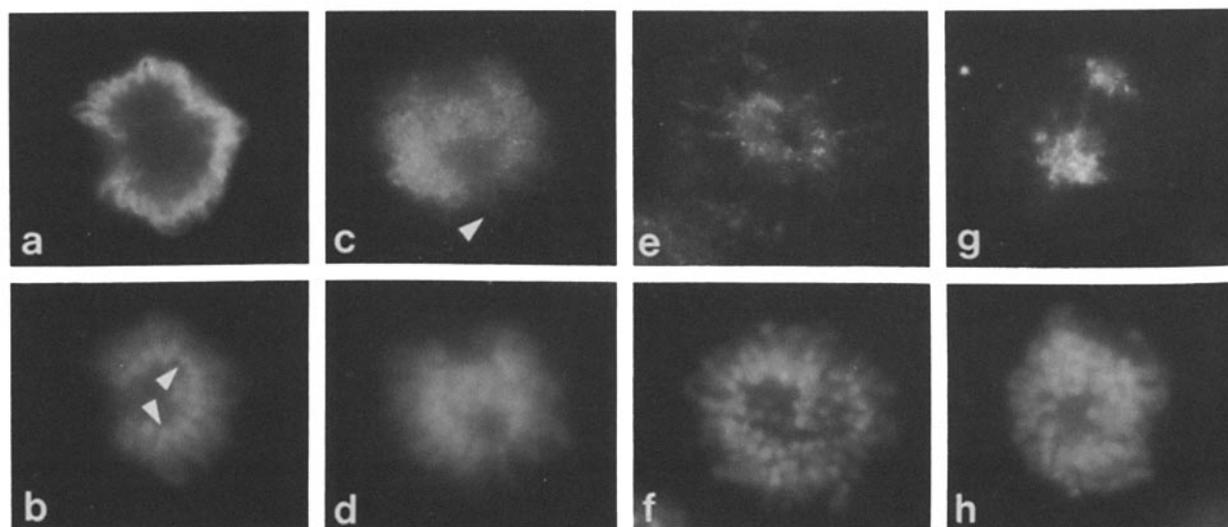
FIGURE 7 Prometaphase nuclei stained with P1 (a), I1 (c), PI1 (e), or PI2 (g) antibodies and counterstained with Hoechst (b, d, f, and h, respectively). (a and b) The chromosomes (b) are oriented radially around a central space with the centromeres (arrows) (see also g–i) towards the center. Antibody P1 stains the periphery of the chromosome mass, coating the projecting chromosome arms. (c and d) Antibody I1 is distributed as specks along the surface of the chromosome (arrowheads). The interior of the chromosome also shows some diffuse fluorescence. (e and f) Antibody PI1 is not chromosome associated. Faint granular fluorescence is visible in the central space of the prometaphase configuration as well as between some chromosomes. (g and h) Antibody PI2 is not chromosome associated. Two foci of stain are evident, resembling the staining of involutions of the nuclear periphery observed in prophase (cf. Fig. 4g). × 1,450.

Prophase

In prophase, the staining intensity with antibody P1 increased manyfold, so that adjacent interphase and prophase nuclei could not be photographed with the same exposure. This elevated staining intensity occurred throughout mitosis. The stained irregular inward projections from the nuclear periphery present in interphase were more numerous in early prophase (Fig. 5, a–c). This was seen most clearly when the inner surface of the nuclei was examined (Fig. 5a). In later prophase (Fig. 6, a and b), the projections were seen to

coincide with the surface of short lengths of condensed chromosomes, coating the chromosomes where they lay at the nuclear periphery. Although condensed chromosomes were evident throughout the entire nucleus by DNA staining (Fig. 6b), only those portions at the periphery of the nucleus were coated with antigen to P1. All chromosomes at the nuclear periphery showed surface staining with P1.

The internal staining of interphase nuclei with antibody I1 was redistributed at prophase (Fig. 6, c and d), apparently associating itself with the condensing chromosomes. In contrast to the staining pattern of P1 (Fig. 6, a and b), all
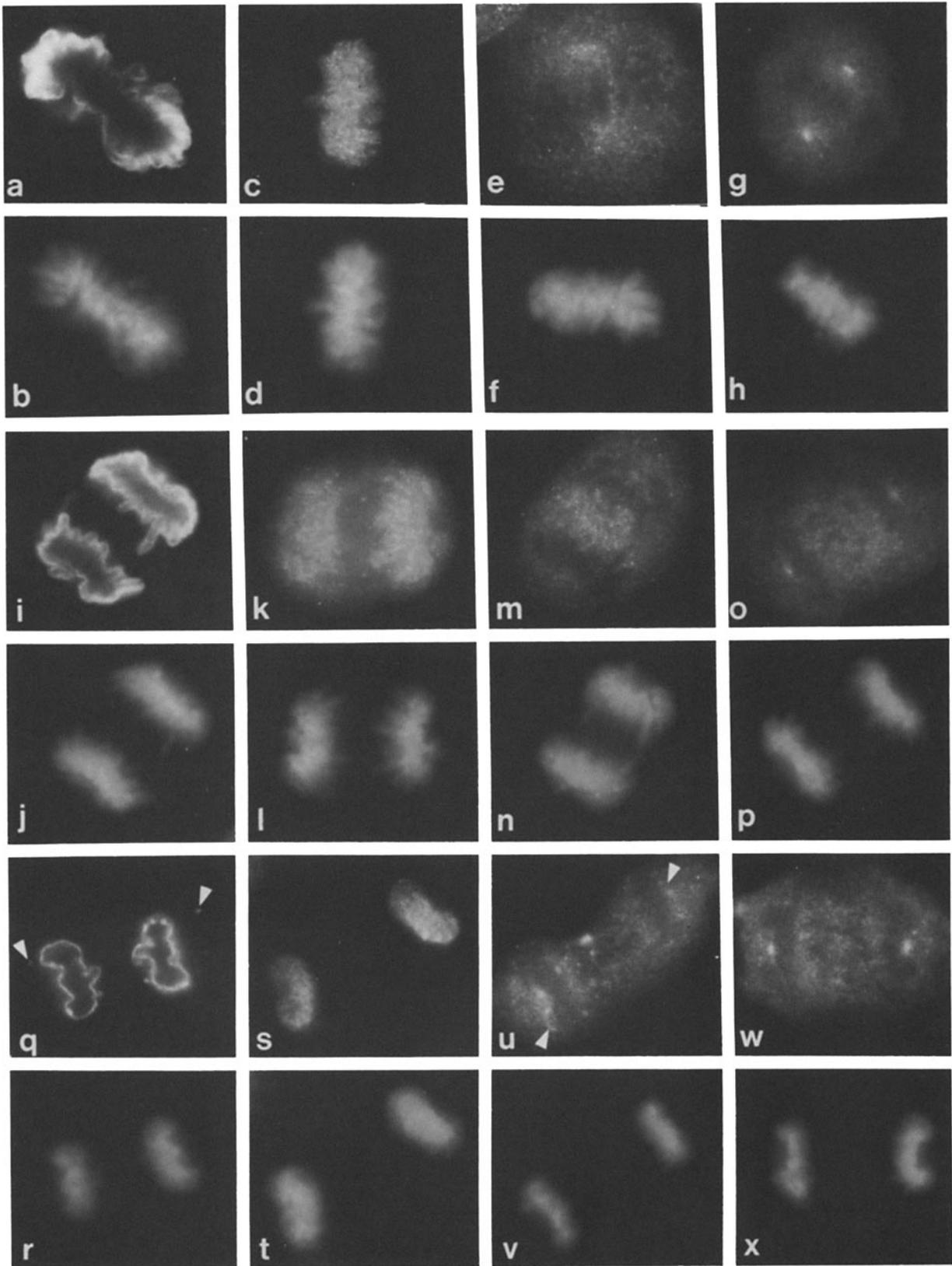
chromosome segments throughout the nucleus were stained with I1. The stain was distributed as specks along the entire surface of each chromosome segment, and there also appeared to be some diffuse staining of the interior of each chromosome.

Early in prophase the staining of the nucleoplasm with antibody PI1 (Fig. 5, d–f) was patchy, indicating clustering of the interphase specks of stain between condensing chromosomes. There was no evidence of any direct association of stain with the chromosomes. Brightly staining granules were observed in the cytoplasm of some prophase cells, usually in two clusters near the surface of the nucleus (Fig. 5, d and e). The peripheral nuclear staining was accentuated later in prophase (Fig. 6, e and f), where two involutions of the nuclear periphery were readily visible (Fig. 6, e and f).

The internal component staining with PI2 became redistributed early in prophase (Fig. 5, g–i), lying in patches between condensing chromosomes. The peripheral staining was no longer granular (Fig. 5h), and the surface appeared "wrinkled" in places. Later in prophase (Fig. 6, g and h), internal staining disappeared and the peripheral staining consisted of bright diffuse fluorescence. As observed with PI1 (Fig. 6, e and f), the nuclear periphery was involuted in two places at prophase (Fig. 6, g and h). No staining of cytoplasmic granules was seen with PI2.

Prometaphase

At prometaphase, P1 was detected only at the periphery of the chromosome mass (Figs. 7a and 10, a, c, and e), closely following the outlines of projecting chromosome arms (Figs. 7b and 10, b, d, and f). No stain was detected within the individual chromosomes or within the chromosome mass. This is illustrated in the through-focus series in Fig. 10, a–f. All chromosome arms at the surface of the configuration (Fig. 10, b and f) were coated (Fig. 10, a and e), but in the midplane of the mass, only those portions of the chromosomes at the periphery (Fig. 10d) were coated by P1 (Fig. 10c). In contrast, prometaphase chromosomes in preparations stained with antilamin were unstained (Fig. 3, a and b). The cytoplasm showed considerable diffuse fluorescence, and in some cells granular bright lines could be seen in places in the cytoplasm around the chromosome mass.

To ascertain that peripheral staining of the chromosome mass by P1 was not simply due to exclusion of antibody, we performed double immunostaining with P1 and antihistone

(Fig. 10, g–h). Although the chromosome mass was only outlined by P1 (Fig. 10g), each chromosome was fully stained by antihistone (Fig. 10h), resembling the pattern recently described with a monoclonal antibody to histone H2b (17).

With antibody I1, a finely granular stain was associated with the surface of the chromosomes at prometaphase (Fig. 7, c and d). There also appeared to be some diffuse staining of the interior of the chromosomes themselves, as had been seen in prophase nuclei (Fig. 6, c and d).

Antibodies PI1 and PI2 were not chromosome associated after nuclear envelope breakdown. Staining with both antibodies was greatly reduced at prometaphase (Fig. 7, e–h). Some specks of stain were visible between chromosomes and in the central space of the prometaphase configuration, perhaps corresponding to the sites of involution of the nuclear periphery observed in prophase.

Metaphase, Anaphase, and Telophase

At metaphase (Fig. 8, a and b), the periphery of the metaphase plate was precisely outlined by P1 (Fig. 8a), with no visible staining of the central portions of the chromosomes. However, any chromosomes lying outside the metaphase plate were individually delineated by P1 (Fig. 8a).

In early anaphase, if the two daughter sets of chromosomes were intertwined, P1 outlined them as one mass. At a more advanced stage of anaphase (Fig. 8, i–j), when the distal ends of the chromosome sets have moved past one another towards the poles, each daughter set of chromosomes was outlined separately by P1 (Fig. 8i). During telophase, the distribution of P1 paralleled the surface irregularities of the condensing chromosome mass (Fig. 8, q and r). In many cells in telophase (Fig. 8q) and in early G1, there were brightly staining globular masses in the cytoplasm.

With antibody I1, the metaphase (Fig. 8, c and d), anaphase (Fig. 8, k and l) and telophase (Fig. 8, s and t) chromosomes were associated along their entire length with bright specks of stain as described for prometaphase. The interior of the chromosomes also showed a diffuse fluorescence.

The PI1 staining was reduced to a diffuse glow of the cytoplasm at metaphase (Fig. 8, e and f) and anaphase (Fig. 8, m and n). As the chromosomes began to lose their individual definition in telophase, a very faint stain could be seen at the periphery of the chromosome mass (Fig. 8, u and v), initially at the side of the mass nearer the spindle poles.

Figure 8   Cells in metaphase (a–h), anaphase (i–p), and telophase (q–x) stained with P1 (a, i, and q), I1 (c, k, and s), PI1 (e, m, and u) or PI2 (g, o, and w) antibodies, and counterstained with Hoechst (b, j, and r; d, l, and t; f, n, and b; h, p, and x, respectively). Metaphase: Antibody P1 stains the periphery of the metaphase plate (a and b) while I1 is seen as fine specks along the chromosomes (c and d). With PI1 (e and f) and PI2 (g and h), the cytoplasm exhibits fluorescence, but no stain is associated with the chromosomes themselves. In cells stained with PI2, stain is also visible in two spots corresponding to the location of the spindle poles (g). Anaphase: Antibody P1 outlined each daughter set of chromosomes (i and j). Antibody I1 is associated with the chromosomes of each daughter set along their entire length (i). The granular nature of the stain, its localization at the surface of the chromosome and the presence of some internal stain are particularly clear in this micrograph. The chromosomes are not stained by PI1 (m and n) or PI2 (o and p) antibodies but the cytoplasm is fluorescent. Some PI2 staining is associated with the spindle poles. Telophase: Antibody P1 (q and r) is localized at the periphery of the chromosome groups, closely outlining the surface irregularities. Brightly staining globular masses are also visible in the cytoplasm (arrowheads). Association of I1 with individual chromosomes is difficult to distinguish (s and t); the stain appears to be evenly distributed throughout the chromosome masses, and the speckling is less clearly evident. Antibody PI1 (u and v) stains the surface of the chromosome masses on the sides closer to the spindle poles (arrowheads), as well as producing a diffuse cytoplasmic fluorescence. With PI2 (w and x), the cytoplasm is faintly stained as are the spindle poles. X 1,450.
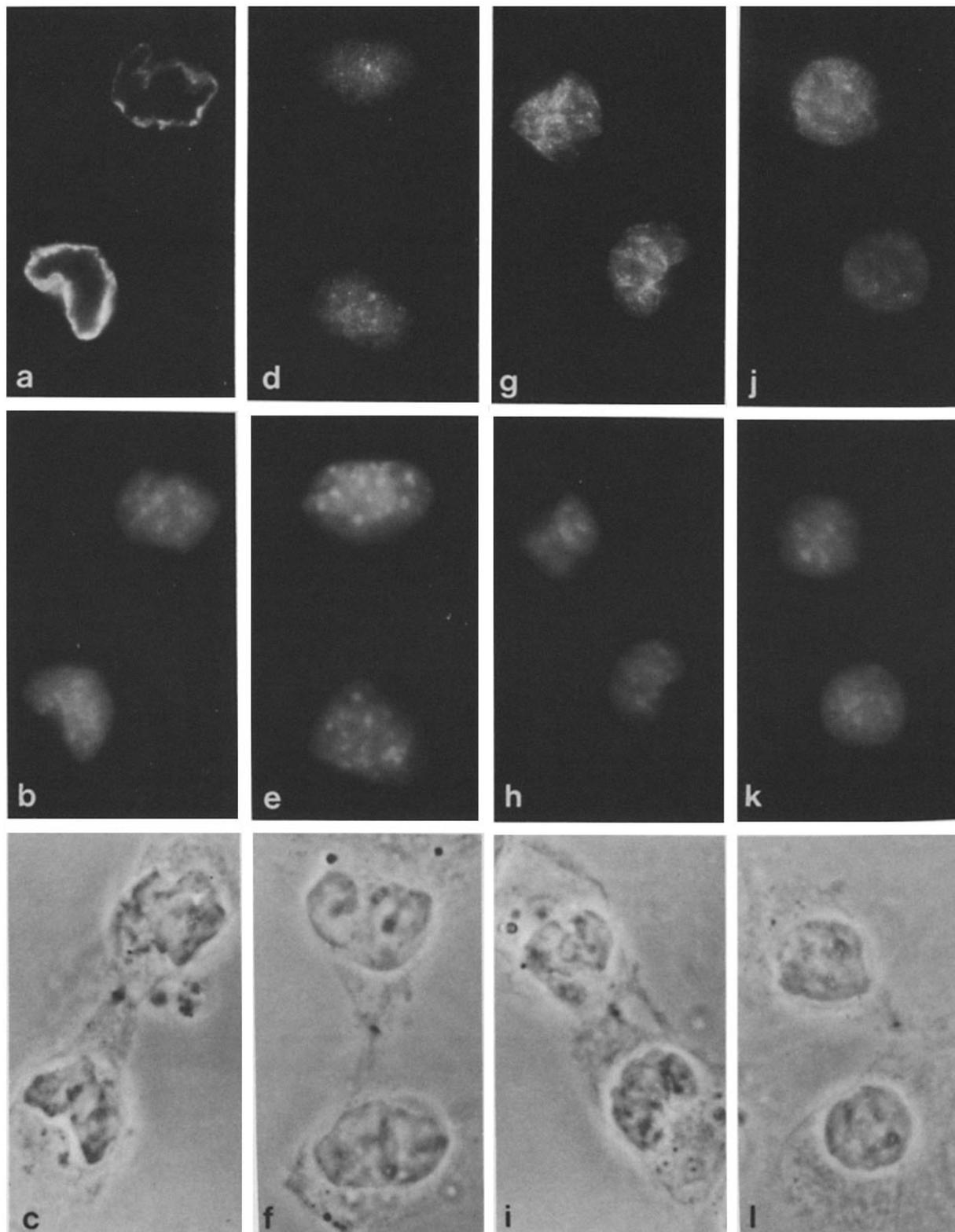
FIGURE 9   Cells in early G1 stained with P1 (a), I1 (d), PI1 (g), or PI2 (j) antibodies, counterstained with Hoechst (b, e, h, and k, respectively), and photographed under phase-contrast illumination (c, f, i, and l, respectively). The midbody is clearly visible in all cells. Although the nuclei are still somewhat irregular in shape (b, d, h, and k), the antibody- and Hoechst-staining patterns are similar to those in nuclei after cytokinesis (cf. Fig. 1). × 1,450.

The chromosomes remained unstained with PI2 during metaphase (Fig. 8, g and h), anaphase (Fig. 8, o and p), and telophase (Fig. 8, w and x) within a diffusely fluorescent cytoplasm. However, two stained spots located at sites appar-

ently corresponding to the spindle poles were visible during these stages (Fig. 8, g, o, and w). At telophase, very faint staining was acquired at the periphery of the chromosome mass (Fig. 8 w).
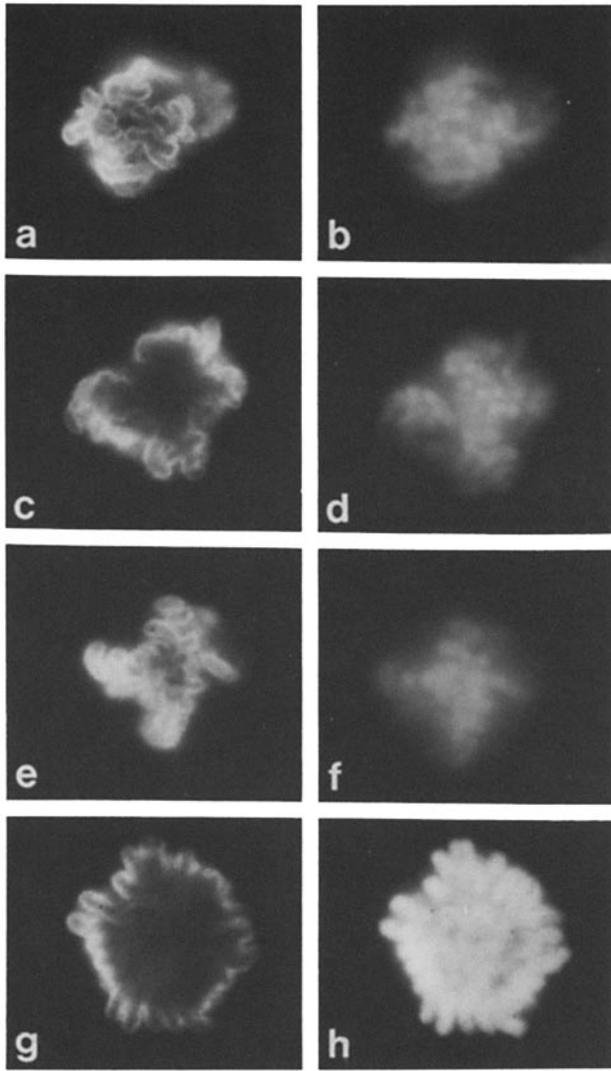
FIGURE 10 (a–f) Through-focus series of cell in late prometaphase stained with antibody P1 (a, c, and e) and counterstained with Hoechst (b, d, and f). When viewed in midplane (c and d) the chromosome mass is closely outlined by P1-staining. The chromosome arms projecting at the top and bottom surfaces of the mass (a and b; e and f) are also fully outlined. The portions of the chromosomes in the center of the chromosome mass (d) are not stained (cf. c and d). (g and h) Cell in early prometaphase stained with P1 (g) and antihistone (h) antibodies. The chromosome mass is outlined by P1 (g), but, at the same plane of focus, each chromosome is fully stained by the antihistone (h). × 1,450.

Early G1

In early G1, the daughter cells were still joined at the midbody (Fig. 9, c, f, i, and l). Some cells showed the antibody-specific staining pattern characteristic of interphase nuclei. Most, however, presented staining patterns intermediate between telophase and interphase.

The staining with P1 was somewhat less bright than earlier in mitosis but was still brighter than after cytokinesis. It was once more peripheral and fairly even in distribution (Fig. 9, a–c).

In parallel with the reappearance of interphase chromatin organization in early G1, the staining by antibody I1 was gradually redistributed throughout the nucleus as bright specks of even size (Fig. 9, d–f).

The peripheral components detected by monoclonals PI1 (Fig. 9, g–i) and PI2 (Fig. 9, j–l) were clearly visible in all early G1 cells. In nuclei showing a relatively diffuse Hoechst stain, similar to that in interphase nuclei (cf. Figs. 9, i and l and 1 c), the internal component was also evident (Fig. 9, g–i).

DISCUSSION

The monoclonal antibodies studied here were generated against a biochemically characterized nuclear fraction, the nuclear matrix (10, 16, 18). They were chosen because they localized antigens of interphase nuclei outside visible chromatin and nucleoli, in distributions paralleling the known location, from electron microscope studies, of different regions of the nuclear matrix, i.e., the pore complex–lamina (P1), the fibrogranular internal matrix (I1), or both (PI1, PI2). Furthermore, we have demonstrated by immunoblotting that three of the four monoclonal antibodies detected polypeptides of the isolated nuclear matrix.

Reports dealing specifically with nuclear matrix antigens are relatively few (19–21), although the distribution of the lamins during the cell cycle and cell differentiation has been extensively investigated (e.g. 14, 22–27). Using the first monoclonal antibodies directed against nonlamin nuclear matrix antigens, we have demonstrated that, whereas the peripheral and internal regions of the nuclear matrix have some common antigens (detected by PI1 and PI2), others (detected by P1 and I1) are restricted to one region or the other. We have also shown that, with the disruption or reorganization of the interphase nuclear matrix during mitosis, the antigens behave independently of one another. Some antigens are dispersed into the cytoplasm, as has been described for the lamins and most other nuclear antigens. Others, however, associate with the chromosomes in characteristic readily distinguishable patterns. These differences in behavior at mitosis may be a reflection of the particular nuclear matrix function in which the antigens are engaged during interphase. The observations with P1 and I1 support a role for the nuclear matrix in the spatial ordering of nuclear processes, a role maintained during mitosis as participation in the structuring of chromosomes.

Monoclonals P1 and I1 were produced against bovine lymphocyte nuclear matrices, whereas monoclonals PI1 and PI2 were made against mouse lymphocyte nuclear matrices. All four antibodies detected antigens in the mouse 3T3 fibroblast cell line, as well as antigens in mouse and bovine lymphocytes. Indeed, antibody P1, for example, detects antigens with similar interphase and mitotic distributions in a number of mammalian, insect, and plant tissues (manuscript in preparation). This suggests that the antigens under investigation are involved in basic nuclear functions common to many organisms.

The antigen detected by P1 is localized at the nuclear periphery during interphase, and numerous studies have shown by immunocytochemistry that the lamins are associated with the nuclear periphery (14, 22, 23, 26). However, from our observations of both interphase and mitotic cells, it is quite clear that the antigens detected by the two antibodies are not the same. The interphase staining with P1 is exclusively peripheral, while the antilamin reveals an internal component not only in our preparations but also in previously published reports (14, 22). At mitosis, whereas the P1 antigen becomes associated with chromosomes, the lamins disperse into the cytoplasm. Furthermore, we have shown by immu-

noblotting that P1 detects an antigen of M_r 27,000–30,000; the lamins have been identified at M_r 60,000–70,000 (14, 22).

Perichromin, a conserved nuclear envelope-associated antigen localized at the periphery of mitotic chromosomes has been recently detected by an autoimmune antibody (28). The antigen has been identified as a single polypeptide of M_r 33,000. Although perichromin is strongly peripheral at interphase in Chinese hamster ovary cells, it is uniformly distributed throughout the nuclei of *Drosophila* cells. The P1 antigen appears to be distinct from perichromin. It is exclusively peripheral in all cell types examined, including insect cells (manuscript in preparation), and detects polypeptides of M_r 27,000–31,000. The monoclonal antibodies PI1 and PI2 also detect components of the nuclear periphery in 3T3 cells. Taken together these data indicate that the nuclear periphery is more complex than previously considered.

We propose that the antigen to P1 may function in the spatial ordering of DNA during interphase, and the spatial ordering of chromosomes during mitosis. Recently, a similar function has been proposed for perichromin (28). Numerous workers have proposed that DNA is spatially ordered during interphase (29–34), and that the order is established by anchoring of interphase DNA loops on the nuclear matrix (33–37). At least some of these loops are anchored at the nuclear periphery (for reviews, see references 32 and 33). The antigen detected by P1 may be involved in anchoring DNA loops, by itself or by interaction with other nuclear proteins, e.g., the lamins.

There is also considerable evidence for spatial order of chromosomes during mitosis, i.e., at the metaphase plate (32, 38). The behavior of the P1 antigen during mitosis is consistent with the notion that it may be implicated in translating interphase order into metaphase order. With the fragmentation of the nuclear envelope at the end of prophase, the P1 antigen, either by itself or in association with yet unknown factors, may remain chromosome associated so as to retain the spatial order present during interphase. It is unlikely that the P1 antigen interacts in a sequence-specific manner with the chromosomes. Considering only the regions of the centromeres, for example, it is clear that, whereas these are not coated by P1 at metaphase, they become associated with P1 during anaphase and telophase. The antigen to P1 may act merely as a physical constraint on the chromosomes, maintaining them in the relative positions established previously. It is interesting to note that Paulson (39) has shown that all the chromosomes from a cell adhere to one another and are isolated as one cluster under appropriate isolation conditions. He suggests that this may reflect suprachromosomal organization in vivo.

The association of the I1 antigen with chromosomes during mitosis and its nonheterochromatin localization during interphase suggest that the antigen may be involved in structural organization of chromosomes both during interphase and mitosis. Since the I1 antigen appears to be localized largely at chromosome surfaces during mitosis, it is unlikely to be a constituent of the internal chromosome scaffold as prepared by Earnshaw and Laemmli (40). However, antigen I1 could be a component of the 25-nm granules recently demonstrated by Engelhardt et al. (41) in interphase nuclear matrices and chromosome scaffolds.

The antigens for antibodies PI1 and PI2 showed similar distributions throughout the cell cycle, but with some characteristic differences. At interphase, the intercellular staining

pattern was relatively consistent wtih PI2, but with PI1, varied considerably in different nuclei. The type of staining displayed by a particular nucleus with PI1 could not be correlated with any unique structure of the nucleus. It may be related to the metabolic state of the cell, perhaps to its position within the cell cycle. Riley and Keller (42) have shown extensive reorganization of a nuclear matrixlike fraction as HeLa cells progress through interphase.

The interphase staining pattern as well as the dissolution and reacquisition of staining at prometaphase and telophase, respectively, suggest some association of the PI1 and PI2 antigens with the nuclear envelope (33). By mid-prophase, monoclonal PI2 showed only an agranular peripheral component. The altered appearance of the peripheral staining could be due to posttranslational modifications of the PI2 antigen similar to changes in the extent of phosphorylation of lamins and nuclear proteins which are known to occur at about this stage of mitosis (27, 43, 44). It may also, however, reflect changes in distribution resulting from the loss (e.g., the lamins) and/or gain (e.g., P1 antigen) of other peripheral proteins during prophase.

REFERENCES

1. Berezney, R. 1979. Dynamic properties of the nuclear matrix. *In* The Cell Nucleus, Vol. VII. H. Busch, editor. Academic Press, Inc., New York. 413–477.
2. Brasch, K. 1984. Drug induced perturbations of the nuclear matrix. *In* The Nuclear Matrix. R. Berezney, editor. Plenum Press, New York. In press.
3. Comings, D. E., and K. E. Peters. 1981. Two-dimensional gel electrophoresis of nuclear particles. *In* The Cell Nucleus, H. Busch, editor. Academic Press, Inc., New York. 89–118.
4. Bekers, A. G. M., H. J. Gijzen, R. D. F. Taalman, and F. Wanka. 1981. Ultrastructure of the nuclear matrix from *Physarum polycephalum* during the mitotic cycle. *J. Ultrastruct. Res.* 75:352–362.
5. Capco, D. G., and S. Penman. 1983. Mitotic architecture of the cell: the filament networks of the nucleus and cytoplasm. *J. Cell Biol.* 96:896–906.
6. Capco, D. G., K. M. Wan, and S. Penman. 1982. The nuclear matrix: three-dimensional architecture and protein composition. *Cell.* 29:847–858.
7. Detke, S., and J. M. Keller. 1982. Comparison of the proteins present in HeLa cell interphase nucleoskeletons and metaphase chromosome scaffolds. *J. Biol. Chem.* 257:3905–3911.
8. Hodge, L. D., P. Mancini, F. M. Davis, and P. Heywood. 1977. Nuclear matrix of HeLa S3 cells: polypeptide composition during adenovirus infection and in phases of the cell cycle. *J. Cell Biol.* 72:194–208.
9. Peters, K. E., T. A. Okada, and D. E. Comings. 1982. Chinese hamster nuclear proteins: an electrophoretic analysis of interphase, metaphase and nuclear matrix preparations. *Eur. J. Biochem.* 129:221–232.
10. Setterfield, G., R. Hall, T. Bladon, J. E. Little, and J. G. Kaplan. 1983. Changes in structure and composition of lymphocyte nuclei during mitogenic stimulation. *J. Ultrastruct. Res.* 82:264–282.
11. Kennett, R. H., T. J. McKearn, and K. B. Bechtol. 1980. Monoclonal Antibodies. Hybridomas: A New Dimension in Biological Analysis. Plenum Press, New York and London.
12. Brasch, K. 1982. Age- and ploidy-related changes in rat liver nuclear proteins as assessed by one- and two-dimensional gel electrophoresis. *Can. J. Biochem.* 60:204–214.
13. Burnette, W. N. 1981. "Western blotting": electrophoretic transfer of proteins from sodium dodecyl sulfate-polyacrylamide gels to unmodified nitrocellulose and radiographic detection with antibody and radioiodinated protein A. *Anal. Biochem.* 112:195–203.
14. McKeon, F. D., D. L. Tuffanelli, K. Fukuyama, and M. W. Kirschner. 1983. Autoimmune response directed against conserved determinants of nuclear envelope proteins in a patient with linear scleroderma. *Proc. Natl. Acad. Sci. USA.* 80:4374–4378.
15. Chaly, N., T. Bladon, W. A. Aitchison, G. Setterfield, J. G. Kaplan, and D. L. Brown. 1983. Redistribution of nuclear matrix antigens during spindle formation. *J. Cell Biol.* 97:189a. (Abstr.)
16. Setterfield, G., R. Hall, T. Bladon, K. Brasch, and J. G. Kaplan. 1983. Changes in structure and composition of lymphocyte nuclei during mitogenic stimulation. Proceedings of the 15th International Leucocyte Culture Conference. John Wiley and Sons, New York.

17. Turner, B. M. 1982. Immunofluorescent staining of human metaphase chromosomes with monoclonal antibody to histone H2b. *Chromosoma (Berl.).* 87:345–357.

18. Chaly, N., G. Setterfield, J. G. Kaplan, and D. L. Brown. 1983. Nuclear bodies in mouse splenic lymphocytes. 2. Cytochemistry and autoradiography during stimulation by concanavalin A. *Biol. Cell* 49:35–44.

19. Wojtkowiak, Z., D. M. Duhl, R. C. Briggs, L. S. Hnilica, J. L. Stein, and G. S. Stein. 1982. A nuclear matrix antigen in HeLa and other human malignant cells. *Cancer Res.* 42:4546–4552.

20. Lydersen, B. K., and D. E. Pettijohn. 1980. Human-specific nuclear protein that associates with the polar region of the mitotic apparatus: distribution in a human-hamster hybrid cell. *Cell.* 22:489–499.

21. van Eekelen, C. A. G., M. H. L. Salden, W. J. A. Habets, L. B. A. van de Putt, and W. J. van Venrooij. 1982. On the existence of an internal nuclear protein structure in HeLa cells. *Exp. Cell Res.* 141:181–190.

22. Gerace, L., A. Blum, and G. Blobel. 1978. Immunocytochemical localization of the major polypeptides of the nuclear pore complex—lamina fraction: interphase and mitotic distribution. *J. Cell Biol.* 79:546–566.

23. Jost, E., and R. T. Johnson. 1983. New patterns of nuclear lamina induced by cell fusion. *Eur. J. Cell Biol.* 30:295–304.

24. Stick, R., and H. Schwarz. 1982. The disappearance of the nuclear lamina during spermatogenesis: an electron microscopic and immunofluorescence study. *Cell Differ.* 11:235–243.

25. Forbes, D. J., M. W. Kirschner, and J. W. Newport. 1983. Spontaneous formation of nucleus-like structures around bacteriophage DNA microinjected into *Xenopus* eggs. *Cell.* 34:13–23.

26. Gerace, L., and G. Blobel. 1980. The nuclear envelope lamina reversibly depolymerizes during mitosis. *Cell.* 19:177–187.

27. Stick, R., and H. Schwarz. 1983. Disappearance and reformation of the nuclear lamina structure during specific stages of meiosis in oocytes. *Cell.* 33:949–958.

28. McKeon, F. D., D. L. Tuffanelli, S. Kobayashi, and M. W. Kirschner. 1984. The redistribution of a conserved nuclear envelope protein during the cell cycle suggests a pathway for chromosome condensation. *Cell.* 36:83–96.

29. Agard, D. A., and J. W. Sedat. 1983. Three-dimensional architecture of a polytene nucleus. *Nature (Lond.).* 302:676–678.

30. Brasch, K., and G. Setterfield. 1974. Structural organization of chromosomes in interphase nuclei. *Exp. Cell Res.* 83:175–185.

31. Brasch, K., V. L. Seligy, and G. Setterfield. 1971. Effects of low salt concentration on structural organization and template activity of chromatin in chicken erythrocyte nuclei. *Exp. Cell Res.* 65:61–72.

32. Comings, D. E. 1968. The rationale for an ordered arrangement of chromatin in the interphase nucleus. *Am. J. Hum. Genet.* 20:440–460.

33. Franke, W. W., U. Scheer, G. Krohne, and E.-D. Jarasch. 1981. The nuclear envelope and the architecture of the nuclear periphery. *J. Cell Biol.* 91(3, Pt. 2):39s–50s.

34. Hancock, R., and M. E. Hughes. 1982. Organization of DNA in the interphase nucleus. *Biol. Cell.* 44:210–212.

35. Benyajati, C., and A. Worcel. 1976. Isolation, characterization, and structure of the folded interphase genome of *Drosophila melanogaster. Cell.* 9:393–407.

36. Pardoll, D. M., B. Vogelstein, and D. S. Coffey. 1980. A fixed site of DNA replication in eucaryotic cells. *Cell.* 19:571–581.

37. Vogelstein, B., D. M. Pardoll, and D. S. Coffey. 1980. Supercoiled loops and eucaryotic DNA replication. *Cell.* 22:79–85.

38. Heslop-Harrison, J. S., and M. D. Bennett. 1983. The spatial order of chromosomes in root-tip metaphases of *Aegilops umbellulata. Proc. R. Soc. Lond. B. Biol. Sci.* 218:225–239.

39. Paulson, J. R. 1982. Isolation of chromosome clusters from metaphase-arrested HeLa cells. *Chromosoma (Berl.).* 85:571–581.

40. Earnshaw, W. C., and U. K. Laemmli. 1983. Architecture of metaphase chromosomes and chromosome scaffolds. *J. Cell Biol.* 96:84–93.

41. Engelhardt, P., Plangens, U., Zbarsky, I. B., and L. S. Filatova. 1982. Granules 25–30 nm in diameter: basic constituent of the nuclear matrix, chromosome scaffold, and nuclear envelope. *Proc. Natl. Acad. Sci. USA.* 79:6937–6940.

42. Riley, D. E., and J. M. Keller. 1978. Cell cycle-dependent changes in non-membranous nuclear ghosts from HeLa cells. *J. Cell Sci.* 29:129–146.

43. Henry, S. M., and L. D. Hodge. 1983. Nuclear matrix: A cell-cycle dependent site of increased intranuclear protein phosphorylation. *Eur. J. Biochem.* 133:23–29.

44. Song, M.-K. H., and K. W. Adolph. 1983. Phosphorylation of nonhistone proteins during the HeLa cell cycle: relationship to DNA synthesis and mitotic chromosome condensation. *J. Biol. Chem.* 258:3309–3318.